NeuroImage: Clinical 4 (2014) 593–603

Contents lists available at ScienceDirect

NeuroImage: Clinical

journal homepage: www.elsevier.com/locate/ynicl

Atypical sulcal anatomy in young children with autism spectrum disorder

G. Auzias[a,*], M. Viellard[a,b], S. Takerkart[a], N. Villeneuve[b], F. Poinso[a,b], D. Da Fonséca[a,c], N. Girard[d,e], C. Deruelle[a]

[a] INT UMR 7289, Aix-Marseille Université, CNRS, France
[b] Centre de Ressources Autisme, Service de Pédopsychiatrie, APHM, Hôpital Ste Marguerite, Marseille, France
[c] Service de Pédopsychiatrie, APHM, Hôpital Salvator, France
[d] CRMBM UMR 7339, Aix-Marseille Université, CNRS, France
[e] APHM Timone, Service de Neuroradiologie Diagnostique et Interventionnelle, Marseille, France

ARTICLE INFO

Article history:
Received 12 December 2013
Received in revised form 18 March 2014
Accepted 19 March 2014

Keywords:
Autism
MRI
morphometry
sulci

ABSTRACT

Autism spectrum disorder is associated with an altered early brain development. However, the specific cortical structure abnormalities underlying this disorder remain largely unknown. Nonetheless, atypical cortical folding provides lingering evidence of early disruptions in neurodevelopmental processes and identifying changes in the geometry of cortical sulci is of primary interest for characterizing these structural abnormalities in autism and their evolution over the first stages of brain development. Here, we applied state-of-the-art sulcus-based morphometry methods to a large highly-selective cohort of 73 young male children of age spanning from 18 to 108 months. Moreover, such large cohort was selected through extensive behavioral assessments and stringent inclusion criteria for the group of 59 children with autism. After manual labeling of 59 different sulci in each hemisphere, we computed multiple shape descriptors for each single sulcus element, hereby separating the folding measurement into distinct factors such as the length and depth of the sulcus. We demonstrated that the central, intraparietal and frontal medial sulci showed a significant and consistent pattern of abnormalities across our different geometrical indices. We also found that autistic and control children exhibited strikingly different relationships between age and structural changes in brain morphology. Lastly, the different measures of sulcus shapes were correlated with the CARS and ADOS scores that are specific to the autistic pathology and indices of symptom severity. Inherently, these structural abnormalities are confined to regions that are functionally relevant with respect to cognitive disorders in ASD. In contrast to those previously reported in adults, it is very unlikely that these abnormalities originate from general compensatory mechanisms unrelated to the primary pathology. Rather, they most probably reflect an early disruption on developmental trajectory that could be part of the primary pathology.

1. Introduction

Autism spectrum disorder (ASD) is a pervasive neurodevelopmental disorder characterized by hampered socialization and communication, with the emergence of stereotyped and repeated behavior (American Psychiatric Association, 2000). The total brain volume is abnormally increased in young children with ASD (Courchesne et al., 2007; Schumann and Nordahl, 2011) supporting the view that this disorder is associated with an atypical brain connectivity resulting from altered trajectory of early brain development (e.g., Belmonte et al., 2004; Schumann et al., 2010). The specific cortical structural underpinnings remain however largely unknown. A confounding factor when comparing brain structures in participants with or without ASD is the complex and heterogeneous pattern of brain maturation. Several studies established that the impact of ASD on brain tissue volumes (Courchesne et al., 2007; Schumann et al., 2010), cortical thickness (Doyle-Thomas et al., 2013; Mak-Fan et al., 2011; Misaki et al., 2012; Raznahan et al., 2010; Scheel et al., 2011; Wallace et al., 2010), or surface area (Hazlett et al., 2011; Mak-Fan et al., 2011; Raznahan et al., 2010) is strongly age-dependent. This confounding factor may partially account for the inconsistencies in voxel based morphometry studies that failed to reach consensus (Amaral et al., 2008; Anagnostou and Taylor, 2011; Chen et al., 2011; Nickl-Jockschat et al., 2012; Stanfield et al., 2008) as illustrated by the alternatively documented increased (Bonilha et al., 2008) or decreased (Toal et al., 2010) gray-matter volume in the medial temporal lobe. In the same

* Corresponding author at: Institut de Neurosciences de la Timone, Faculté de Médecine, 27, Boulevard Jean Moulin, 13385 cedex 5 Marseille, France.
E-mail address: guillaume.auzias@gmail.com (G. Auzias).

2213-1582/$ - see front matter
http://dx.doi.org/10.1016/j.nicl.2014.03.008

vein, vertex-to-vertex surface-based morphometry reported opposite changes in cortical thickness in the frontal, parietal and temporal lobes when comparing ASD to controls (Doyle-Thomas et al., 2013; Ecker et al., 2010; Hadjikhani et al., 2006; Hyde et al., 2010; Misaki et al., 2012; Raznahan et al., 2013; Stevenson, 2012; Wallace et al., 2010). Searching for changes in cortical surface area in ASD also led to conflicting results (Hazlett et al., 2011; Raznahan et al., 2013; Wallace et al., 2013).

Hence, the pattern of brain development impairment in ASD requires clarification in terms of both localization and timing. A promising approach to elucidate this issue is to consider the shape of the cortical surface. Cortical folding begins in utero and continues during childhood and adolescence (Mangin et al., 2010; White et al., 2010) and is thought to reflect an ongoing process of myelination and synaptic remodeling (Casey et al., 2005; Su et al., 2013; White et al., 2010). Moreover, changes in the geometry of the cortical surface may reflect long-standing developmental influences of mechanical tension along axons on the folding process (Van Essen, 1997). Atypical folding may thus reflect the signature of perturbations in the development of brain connections and provide lingering evidence of early or late disruptions of neurodevelopmental processes (J. Dubois et al., 2008a). The preliminary work of Hardan et al. (2004) showed an increased gyrification in ASD on one 2D coronal slice. Using more advanced computation of gyrification on the cortical surface extracted from 3D images, Kates et al. (2009) and Wallace et al. (2013) also revealed increased folding in ASD compared to typically developing individuals, mostly located in the frontal, parietal and temporal lobes. Consistent results have been reported using geometrical descriptors such as curvedness and shape index (Awate et al., 2008), convexity, curvature and metric distortions (Ecker et al., 2010). Nordahl et al. (2007) demonstrated increased depth in the operculum and the intraparietal sulcus for participants with ASD compared to typically developing individuals. These studies shed some light on the atypical geometry of the cortical surface in ASD but their interpretation is limited since they did not capture the fact that folding is an *organized* process.

Indeed, early brain maturation and folding is a process in which some folds appear systematically before others (e.g., Chi et al., 1977; Garel et al., 2001; Hansen et al., 1993; Jessica Dubois et al., 2008b). It is thus critical for understanding typical and atypical brain development to consider the cortical shape through the representation of the folds as a set of cortical sulci that are organized across the surface in space (i.e., their respective location is consistent such as whether the superior frontal sulcus is systematically located anterior to the central sulcus) and time (i.e., their appearance and expansion during brain maturation is in order such as whether for instance the central sulcus appears before the superior frontal sulcus). On the theoretical level, sulcus-based morphometry (Mangin et al., 2004a, 2004b, 2004c) differs from the other techniques described above because cortical sulci are considered as organized entities, while all cortical vertices or voxels are considered as equally important in surface-based and voxel-based approaches.

Sulcus-based morphometry benefits from recent methodological efforts concerning the extraction and analysis of the shape of cortical sulci. Multiple shape descriptors are computed for each sulcus, hereby distinguishing the folding measurement into distinct factors such as the length and depth of the sulcus. Due to the geometrical complexity and the variability of cortical folds across subjects, fine-scale sulcus-based morphometry is challenging, but these difficulties can be overcome by combining modern automatic segmentation algorithm (Mangin et al., 2004a) with expert manual identification of sulci. Notably, sulcus-based morphometry has already been proven to be sensitive to psychiatric syndromes such as schizophrenia (Cachia et al., 2008; Penttilä et al., 2008) and bipolar disorders (Penttilä et al., 2009). Moreover, recent studies demonstrated age-related changes in the geometry of sulci at the lobular scale in adolescents (Alemán-Gómez et al., 2013) as well as in elderly (Im et al., 2008). Altogether, these studies advocate that the geometry of cortical sulci is a particularly well-suited tool to describe brain morphology in neurodevelopmental disorders such as ASD.

To our knowledge, only one publication has investigated the role of sulci in ASD using manual identification (Levitt et al., 2003). In this work, the authors created variability maps of 11 sulci manually traced on each hemisphere. They reported that an anterior and superior shift in the Sylvian fissure, superior temporal sulcus, and inferior frontal sulcus characterized the children with ASD. However, this study used small cohorts of ASD adolescents, mixing males and females while the gender effects on brain shape are known to be prominent for healthy (Raznahan et al., 2011) as well as for autistic individuals (Calderoni et al., 2012; Lai et al., 2013). They also reported statistics that were uncorrected for multiple comparisons.

In this study, we expect to find localized deficient architecture in the ASD group confined to regions that are functionally relevant with respect to cognitive processes assumed to be altered in autism i.e., emphasizing disruption of verbal and non-verbal communication and social interactions, such as the prefrontal and parietal cortex (Schumann and Nordahl, 2011; Verhoeven et al., 2010). In order to successfully demonstrate the effects of ASD on cortical shape using sulcal-base morphometry, we reason that 1) the cohort of patients and control participants should include children as young as possible with a narrowly select patient phenotype 2) manual sulcus labeling is required to obtain reliable between subjects association in e.g., frontal and parietal regions, 3) diagnosis group and age effects on shape descriptors should be treated in the same work, and 4) the gender effect on sulcal morphology should be avoided through gender specific study. The present work is a novel study involving a large cohort of 59 young male children (18–108 months) specifically diagnosed with autistic disorder and 14 well-matched control children. All brain scans were acquired with high-resolution anatomical MRI acquired on a single 1.5 T MR scanner, resulting in a highly homogeneous database. Several different sulcal shape descriptors were extracted after manual identification by a single experienced investigator, which minimized the risk of criterion variation across cases. We also decided to apply stringent statistical correction for multiple comparisons. These descriptors were compared between ASD and control groups across ages for evaluating developmental trajectories in typically developing and ASD children. In the latter group, these indices were also compared across neurobehavioral scores to demonstrate a link between sulcal shapes and ASD severity.

2. Materials and methods

2.1. A new cohort of young children

MRI data analyzed in this work are part of an ongoing clinical evaluation. Selected participants were 59 young children with autistic disorders (AUT) and 14 control children (CTR). The two groups were matched by age (AUT: 57.4 month-old (19.2), CTR: 57 month-old (19.8), $t = -0.08$, $p = 0.936$) and total brain tissue volume (AUT: 1,116,900 cm^3 (11,813), CTR: 1,115,324 cm^3 (24,252), $t = -0.058$, $p = 0.953$, see Table 2). All participants underwent an extensive clinical interview conducted by two experienced clinicians (NV & MV). All data were recorded using the same imaging parameters and within the same scanner. The study was approved by the local Hospital Ethics Committee, and explicit informed consent was waived according to French legislation because all imaging and clinical data were generated during routine clinical workup and were retrospectively extracted for the purpose of this study.

All 59 participants with AUT met the Diagnostic and Statistical Manual-IV-TR (American Psychiatric Association, 2000) diagnostic criteria as assessed by an experienced clinician. Diagnosis was confirmed using a combination of the Autism Diagnostic Observation

Table 1
AUT group characterization. Note that mean values for intelligence and psychometric scales are not given because the scales to be used were depending on participant age.

Scores	Mean (std)	Range
ADOS	17.4 (3.44)	8–23
ADOS communication	6.24 (1.46)	4–10
ADOS social interaction	11.21 (2.46)	4–15
ADOS stereotyped behavior	2.85 (1.49)	0–7
ADI social interaction	18.59 (4.49)	10–26
ADI communication	11.03 (3.24)	6–21
ADI restricted interests /repetitive behaviors	3.98 (1.82)	0–12
CARS	35.01 (3.85)	26.5–47.5
Vineland	58.51 (9.05)	36–76.5
Vineland communication	55.75 (9.29)	32–78
Vineland daily living skills	58.11 (12.23)	20–79
Vineland socialization	59.88 (6.40)	48–81

Table 2
Global measures.

	AUT	CTR	CTR–AUT
White-matter volume (mm^3)	383,208 (44,719)	396,779 (73,902)	$t = 1.173$ $p = 0.244$
Gray-matter volume (mm^3)	733,934 (53,798)	717,526 (86,563)	$t = -0.921$ $p = 0.359$
Total tissue volume (mm^3)	1,116,900 (11,813)	1,115,324 (24,252)	$t = -0.058$ $p = 0.953$
GSL left (mm)	3895.6 (266.3)	3804.8 (213.6)	$t = -1.359$ $p = 0.186$
GSL right (mm)	3943.0 (242.9)	3904.6 (176.9)	$t = -0.675$ $p = 0.505$
GMD left (mm)	13.34 (0.40)	13.18 (0.39)	$t = -1.236$ $p = 0.220$
GMD right (mm)	13.25 (0.36)	13.15 (0.41)	$t = -0.897$ $p = 0.372$
GSI left (surface ratio)	1.52 (0.10)	1.47 (0.08)	$t = -1.811$ $p = 0.074$
GSI right (surface ratio)	1.56 (0.09)	1.52 (0.08)	$t = -1.569$ $p = 0.121$
GSI (average of left and right)	1.54 (0.01)	1.49 (0.02)	$t = -1.182$ $p = 0.094$

Schedule—Generic (ADOS-G (Lord et al., 2000)) and the Autism Diagnostic Interview—Revised (ADI-R, (Rutter et al., 2003)) administered by a trained clinician (MV). Moreover, the Childhood Autism Rating Scale (CARS, (Schopler et al., 1986)) was obtained for all patients, providing a measure of the severity of autistic behaviors. All AUT participants fulfilled the DSM-IV diagnostic criteria for autistic disorder. Exclusion criteria for the AUT group included Asperger's syndrome, childhood disintegrative disorder and pervasive developmental disorder not otherwise specified or any known comorbid medical conditions, such as fragile X syndrome or other genetic disorders as well as any form of brain injury. AUT children received a wide-covering neuropsychological assessment (see Table 1) by a chartered neuropsychologist, including IQ full-scale score with the Wechsler intelligence scales (WPPSI-III; WISC-IV), Psychoeducational Profile (PEP III or PEP-R depending on the age); standardized psychomotor evaluations, and the Vineland Social Adaptive Behavioral Scales (VABS (Sparrow et al., 1984)).

In order to ensure that all data were recorded using the same acquisition parameters and in the same scanner, the fourteen male control children were obtained through retrospective selection within the database of children referred to Children Timone Hospital for brain MRI with anesthesia. They met the following inclusion criteria: no mental retardation; normal developmental history; attendance of a regular school; no history of seizures or head injury; uncomplicated single birth between 37 and 42 weeks; no diagnosis of major psychiatric, depressive or learning disorder in participant; no pre-existing neurological conditions or major head trauma; and normal imaging as judged by an expert neuroradiologist (NG). All children underwent a detailed diagnostic interview conducted by a research-reliable clinician. They were moreover assessed for neuropsychological exclusionary criteria based on clinical judgment of age appropriate behaviors.

2.2. Imaging protocol and parameters

It has been previously shown that volumetric measurements of both total brain and sub-regions can differ significantly between acquisition scanners (Lotspeich et al., 2004). In order to study the shape of the cortical surface on a fine scale it is thus essential to work on a single-site cohort. In this study, participants were scanned on the same 1.5 T Siemens symphony upgraded TIM scanner of the La Timone University Hospital in a clinical setting. The imaging data for the control children were generated during the same routine clinical workup as patients. In particular, all children were scanned under deep sedation by mask induction with cevoflurane and anesthesia maintenance with intravenous propofol and with an injection of gadolinium. All injections were performed by board-certified clinical experts.

The clinical examination included the acquisition of two high-resolution 3D full-brain anatomical MRIs. The first set was obtained from a 3D T1 inversion recovery (IR) sequence with 1.1 mm isotropic resolution acquired in the sagittal plane (160 slices, 1.1 mm slice thickness, 226 × 256 acquisition matrix, TR = 4000 ms, TE = 407 ms, TI = 350 ms). The second set was obtained after gadolinium injection with 1 mm isotropic resolution 3D gradient echo T1 sequence (MPRAGE) acquired in the sagittal plane (160 slices, 1 mm slice thickness, 256 × 256 acquisition matrix, TR = 1880 ms, TE = 2.92 ms, flip angle = 15). These two scans are respectively denoted as IR and T1 in the following.

2.3. Brain morphometry analysis

Below we describe the procedure used to process brain scans and extract morphological features.

2.3.1. Extraction of the morphometric descriptors: segmentation of brain tissues and sulci

Three of the most widely distributed segmentation software (SPM8, Freesurfer and BrainVISA) were used in our procedure. None of the three techniques was able to successfully segment the T1 volume because of the high intensities corresponding to the cerebral vessels due to the injection of gadolinium. Despite their very good contrast, these pipelines also failed on the IR images because of high values in the background. We therefore developed a dedicated segmentation pipeline by combining the three different software suites in order to cumulate their respective strengths.

As illustrated in Fig. 1, this pipeline was composed of four steps (detailed in Supplementary materials S1). Briefly, the two native MRI scans were denoised using VBM8 (step 1) before cerebrospinal fluid and gray and white-matter were segmented in a mutli-modal setting using SPM8 (step 2). The tissue probability maps were then combined in order to extract the brain from the IR volume that had a better contrast than T1. The extracted brain was then given as input to Freesurfer in order to obtain binary masks of gray and white-matter as well as pial and white surfaces (step 3). The binary gray and white-matter masks were then imported into the BrainVISA segmentation pipeline that is specifically designed to extract cortical sulci as a set of 3D objects (step 4).

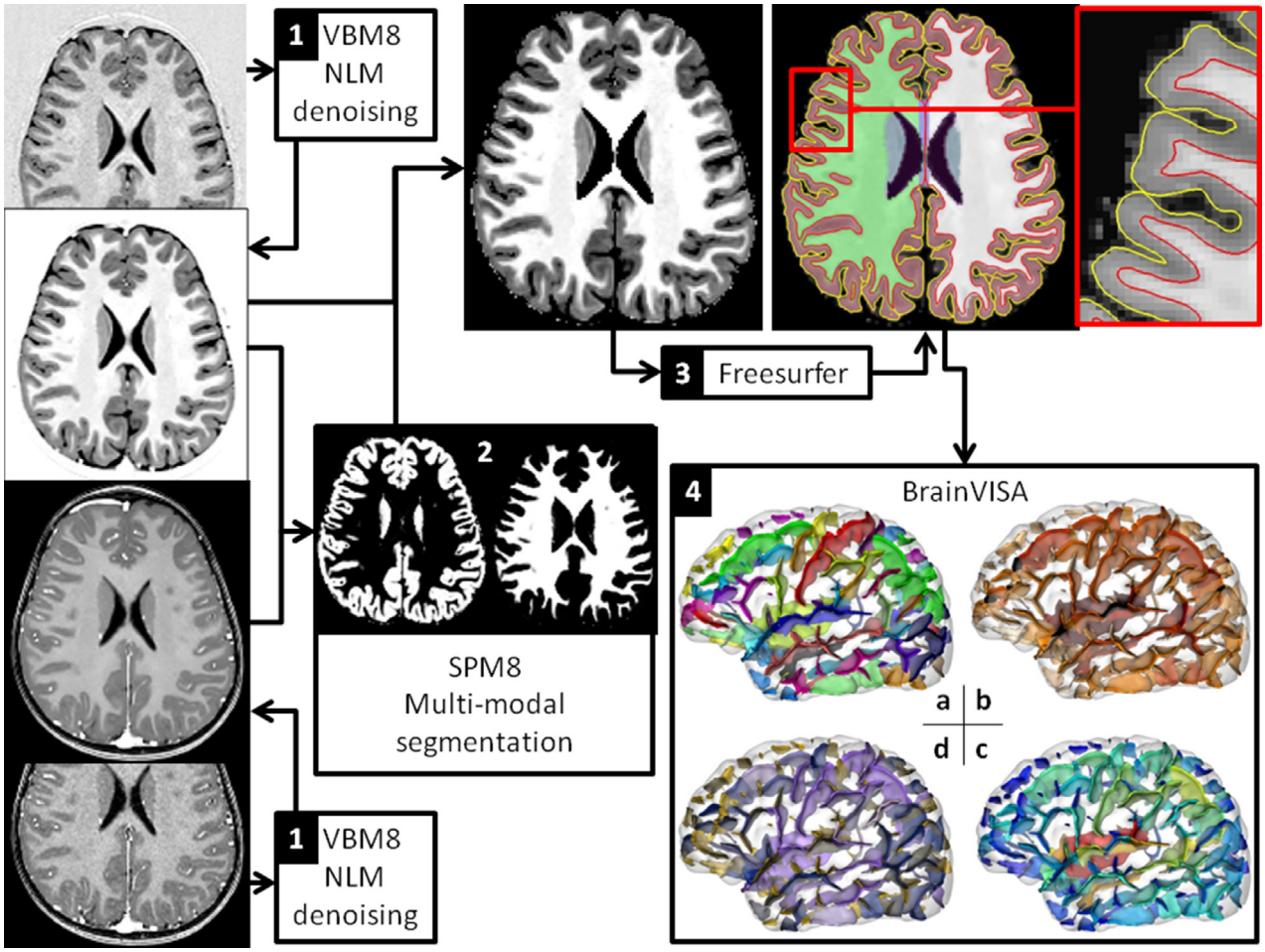

Fig. 1. A dedicated segmentation pipeline was developed by combining VBM8, SPM8 (http://www.fil.ion.ucl.ac.uk/spm/software/spm8/), Freesurfer (http://surfer.nmr.mgh.harvard.edu/) and BrainVISA (http://brainvisa.info/index.html) in order to cumulate their strength. It results in a set of sulcal pieces, each sulcal part being associated with a set of shape descriptors. The 4 steps are detailed in the text and supplementary materials and the sulcal attributes are illustrated in panel 4: sulcal pieces that are colored following a) anatomical denomination, b) mean depth, c) maximum depth and d) area of the folds.

2.3.2. Extraction of the morphometric descriptors: manual sulcus labeling procedure

With the help of BrainVISA, sulci can be automatically identified according to a predefined anatomical nomenclature of 59 sulcus labels per hemisphere (Perrot et al., 2011). The rater agreement between the automatic and human experts reaches 86% on average but performance varies across brain regions, in relation with the inter-individual anatomical variability. Error rate is minimal for well-defined folds such as the central sulcus and is maximal across regions that exhibit greater inter-individual geometrical variations such as the frontal and parietal lobes where it can reach 25% (Perrot et al., 2011). Since these regions are known to be of particular interest in the autistic spectrum disorders (e.g., Chen et al., 2011) relying on fully automatic labeling procedure is not suitable to study the shape of sulci in this pathology. In the present study, the automatic sulcus labeling was thus manually corrected when necessary by an expert (G.A.) that was blind to all phenotypical data, including age and diagnosis.

In order to increase the reproducibility of sulcus labeling across individuals, the expert corrected the sulci of five subjects in parallel (five brains are visualized on the same screen), and refined the resulting labeling by reviewing all the subjects at least three times with four other brains picked randomly across the cohort. Moreover, the expert used the finest-scale nomenclature which corresponds to 59 labels per hemisphere, keeping in mind that the labels could be concatenated a posteriori when the ambiguity due to the observed variability was too important. For instance, the expert had the possibility to make a distinction between the anterior and posterior parts of the inferior temporal sulcus but he reported a low confidence in his ability to make this distinction, such that those two labels were finally fused into an inferior temporal sulcus label that was more reliable. Using this approach, the sulcal pieces were grouped into a set of 21 sulci robustly labeled in each hemisphere, hereby covering all brain regions. The nomenclature of the sulci studied in this work is detailed in Fig. 2A.

2.3.3. Morphometric measures: sulcal shape descriptors

Analyzing the geometry of the cortex through sulcus-based morphometry allows to dissociate distinct and complementary components in the geometry of a sulcus. Several descriptors of the shape of each sulcus piece are computed during the segmentation as illustrated in Fig. 2, see Mangin et al. (2004a) for details. In the present study, we focused on the following four parameters that are illustrated in Fig. 2 for the left central sulcus. The sulcal index (SI) is an estimation of the local cortex folding and is defined as the ratio between the area the sulcus and the area of the brain hull. Because SI is based on area measurements, it is related to the gyrification index (Schaer et al., 2008) and the surface ratio (Toro et al., 2008) which are computed in every vertex of the cortical surface. Although Awate et al. (2008) and Wallace et al. (2013) reported abnormalities in autistic spectrum disorders using such descriptor, it may suffer from a lack of sensitivity. Indeed, a reduced depth associated with an increased length (or

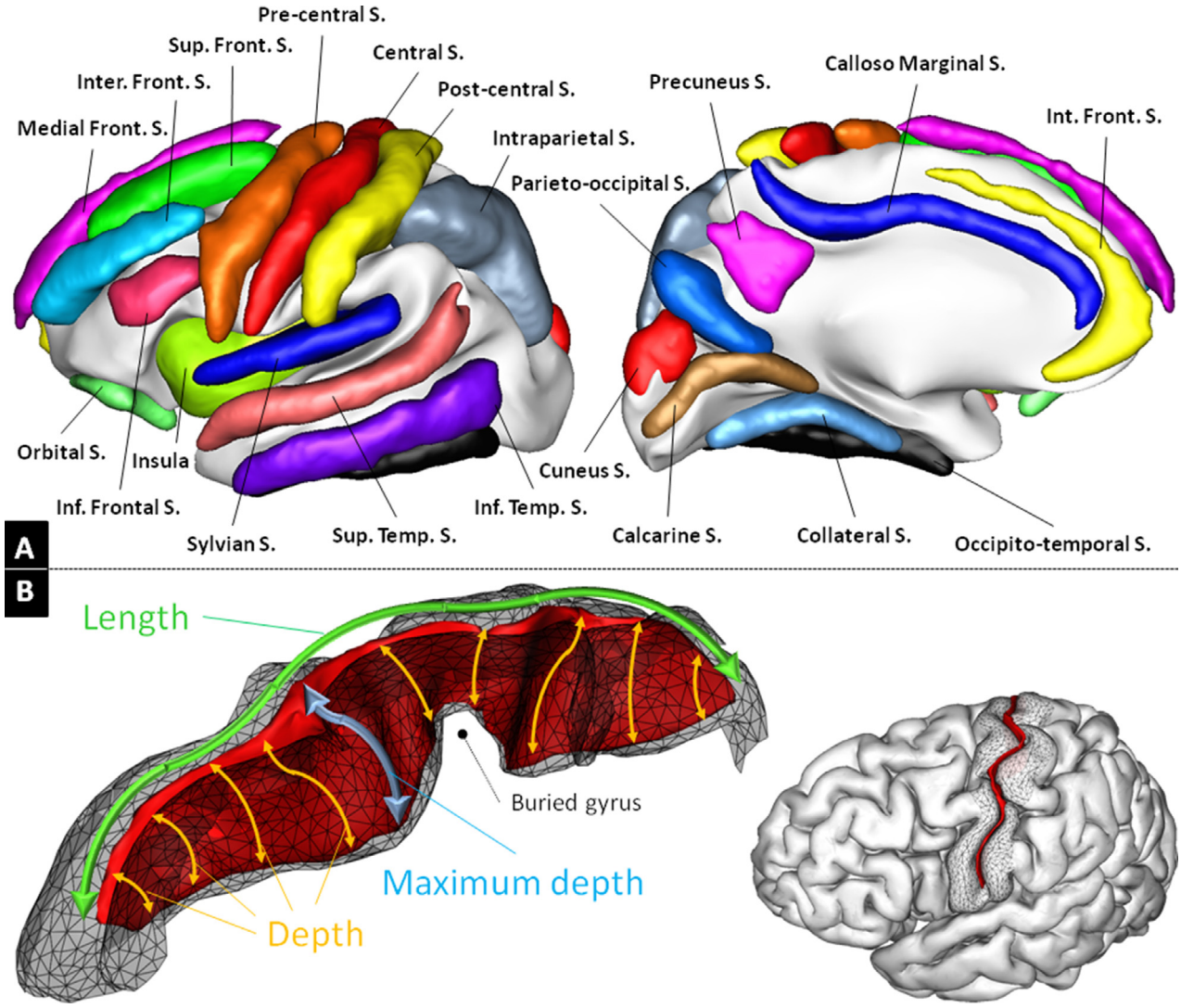

Fig. 2. Illustration of the sulcal nomenclature and shape descriptors used in the current work. A) The nomenclature of sulci used in this study. It can be compared with the finest-scale nomenclature of 59 sulcal pieces available in BrainVISA (*http://www.lnao.fr/IMG/png/brainvisa_sulci_atlas_with_table_150dpi-r90.png*). B) Illustration of the sulcus shape descriptors used in this work for the left central sulcus of an individual. The depth of the central sulcus is known to vary, due to the presence of a buried gyrus (Cykowski et al., 2008). The depth is computed for each point at the bottom of the fold as the distance to the hull, following the sulcus (in orange). The mean depth is the average of the depth across all bottom points and the maximum depth corresponds to the maximal value (in blue). The length is illustrated in green and the area of the sulcus corresponds to the area of the sulcus tessellation shown here as a red ribbon.

vice-versa) will not result in detectable difference in SI. Hence, we advocate that area-related descriptors may be advantageously replaced by the combination of the following length and depth descriptors as described hereafter in order to detect subtle differences related to neurodevelopmental pathologies such as the autism spectrum disorders. The *length* of a sulcus is measured as the geodesic length of the junction between a sulcus and the hull of the brain. The *mean depth* relates to the average of the depth of all the voxels that correspond to the bottom of a sulcus (the depth of a voxel is defined as the geodesic distance along the sulcus to the brain hull). The *maximum depth* is the maximum of the depth across all the bottom voxels of a sulcus, see Fig. 2 for illustration. As discussed in Section 4, the combination of length, mean depth and maximum depth is of particular interest in the context of developmental disorders.

In addition, 3 global descriptors were computed by summing these sulcal indices across all cortical folds of each hemisphere: a *Global Sulcal Index* (*GSI*) corresponding to the ratio between the outer surface of the brain and the surface hidden in the folds, a *Global Sulcal Length* (*GSL*), which is the sum of the sulcus lengths and a *Global Mean Depth* (*GMD*) which is the mean depth obtained across sulci. All morphometric measurements and especially combinations across fold pieces were done using the dedicated tool in BrainVISA. In particular, mean depth was averaged with weights relative to the length of sulcal pieces.

2.3.4. Morphometric measures: volumetric measurements

We also computed the volumes of gray- and white-matter and total brain tissue volume (sum of gray- and white-matter) as provided by Freesurfer. While not being the main focus of this work, global volume differences between AUT and CTR have to be taken into account since brain folding is known to be related to its volume (Germanaud et al., 2012; Toro et al., 2008) and early brain overgrowth has been consistently reported in autism spectrum disorders (e.g., Courchesne et al., 2007).

2.4. Statistical analysis

The sulcal shape descriptors were computed in standardized MNI space and are thus implicitly normalized for inter-individual variations in global brain size and volume. Therefore, global volumetric measurements were not included as covariates in the statistical model. Outliers in sulcal descriptors were identified by both visual inspection and using a Z-score threshold at 2.5 and then removed from the final sample of data ($N = 2.4\%$). Each sulcal shape descriptor was then analyzed for each hemisphere using the following linear model:

$$\text{Descriptor} = \text{Intercept} + \beta_1\ \text{Age} + \beta_2\ \text{Group} + \beta_3 \times \text{Group} + \text{Residuals}.$$

For each descriptor, separate within group analyses were performed when a significant age by group interaction was reported. In the absence of a significant age by group interaction, a simpler model including only the main effect of age and group was used. The main effect of group was tested using the Wilcoxon–Mann–Whitney nonparametric test. All statistical tests were done using the JMP SAS software (*http://www.jmp.com/*). More considerations regarding the issue of unbalanced data samples in our statistical setup are given in Supplementary materials S2.

Statistical significance of the age by group term was assessed using a $p < 0.05$ threshold. In order to control for multiple comparisons in group differences for sulcal descriptors, we applied a conservative Bonferroni correction such that the difference was considered as significant if the p-value was inferior to $0.0023 = 0.05/21$ (21 sulci included in the analysis). In the following, we note p for uncorrected p-values and p_{BC} for corrected p-values ($p_{BC} = 21 \times p$).

3. Results

We first present the results for global morphometric measures before documenting the effects of group and age on sulcus descriptors and their relationship with neurobehavioral measures.

3.1. Global measures

We did not detect any significant difference in global features between AUT and CTR (all $p > .05$, see Table 2) and none of them yielded a significant age by group interaction. The GSI showed an interesting trend towards higher folding in AUT in the left hemisphere. Merging left and right hemisphere by averaging did not result in significant difference.

3.2. Local sulcal descriptors: differences between AUT and CRT

Results of the between group difference for the sulcal shape descriptors are illustrated in Fig. 3. Findings presented in this section were obtained using the statistical model including only the main effects of age and group as none of the descriptors that showed a significant age by group interaction was associated with a significant main effect of group (all $p > .05$). All reported effects are significant after Bonferroni correction, except otherwise specified.

The left superior frontal sulcus (max depth $p = 0.0315$), left inferior temporal (max depth $p = 0.0182$), right medial frontal (max depth $p = 0.0192$), right cuneus (max depth $p = 0.0091$, SI $p = 0.0165$, mean depth $p = 0.0046$), right internal frontal (length $p = 0.0245$) and bilateral orbital sulci (right: max depth $p = 0.0218$, left $p = 0.0234$) showed a non-significant trend towards larger folds in AUT compared to CTR. Strikingly, only three sulci out of the 21 remained in the stringent threshold corresponding to Bonferroni correction : the *right intraparietal*, the *left medial frontal* and the *left central sulci* showed significant difference between AUT and CTR. For the right intraparietal sulcus, mean depth was greater in the AUT compared to the CTR group ($p = 0.0007$, $p_{BC} = 0.0147$), max depth, SI nor length reached statistical significance (all $p > .05$ uncorrected). For the left medial frontal sulcus, length ($p = 0.0016$, $p_{BC} = 0.0336$) and max depth ($p = 0.0005$, $p_{BC} = 0.0105$) were significantly higher for CTR than for AUT. A trend towards larger sulcal index ($p = 0.0086$) for CTR compared to AUT was also observed for this sulcus. Finally, the central sulcus was significantly longer in CTR than in AUT ($p = 0.0006$, $p_{BC} = 0.0126$). An opposite pattern was found for both the max depth and the mean depth where a trend towards deeper sulcus in AUT compared to CTR was observed (max depth $p = 0.0070$ and mean depth $p = 0.0179$).

Table 3
Statistics for age by group interactions and within group effect of age.

Sulcus	Age × group	Within group: AUT	Within group: CTR
SI right post central	$p = 0.0225$	$r^2 = 0.00$, $p = 0.91$	$r^2 = 0.31$, $p = 0.0369$
SI right inferior temporal	$p = 0.0429$	$r^2 = 0.06$, $p = 0.052$	$r^2 = 0.11$, $p = 0.23$
Length right intraparietal	$p = 0.0308$	$r^2 = 0.04$, $p = 0.59$	$r^2 = 0.23$, $p = 0.08$
Length right calcarine	$p = 0.0260$	$r^2 = 0.005$, $p = 0.57$	$r^2 = 0.69$, $p = 0.0004$
Length left superior temporal	$p = 0.0073$	$r^2 = 0.005$, $p = 0.59$	$r^2 = 0.49$, $p = 0.0069$
Max depth right internal frontal	$p = 0.0094$	$r^2 = 0.003$, $p = 0.64$	$r^2 = 0.32$, $p = 0.0324$
Men depth left medial frontal	$p = 0.0146$	$r^2 = 0.04$, $p = 0.114$	$r^2 = 0.18$, $p = 0.122$

3.3. Local sulcal descriptors: differences in age by group interaction

The statistical analysis of the age by group interaction revealed that several sulcal shape descriptors correlated differently with age for AUT compared to CTR children. As can be observed in Fig. 4, two sulci in the left hemisphere and five sulci in the right hemisphere showed a significant age by group interaction. Corresponding statistics are reported in Table 3, including the within group effect of age. In the CTR group, we observed a positive correlation for the mean depth of the left medial frontal sulcus, the length of the left superior temporal sulcus and the max depth of the right internal frontal sulcus, and a negative correlation for the length of the right intraparietal sulcus, the sulcal index of the right postcentral sulcus, the length of the right calcarine fissure and the sulcal index of the right inferior temporal sulcus. By contrast, for all these descriptors, the correlation in the AUT group was not only nonsignificant but also very small ($r^2 < 0.5$). Note that this observation is not due to the difference in the number of subjects involved in each group. The significant correlations were all found in the smaller group of 14 CTR and no significant interaction with age was found in the group of 59 ASD children.

3.4. Correlation between shape descriptors and behavioral assessments

We found several significant correlations between the sulcal shape descriptors that were different between groups and the psychological tests used for the diagnostic in the AUT group. For the left central sulcus, we found a positive correlation between mean depth and ADOS stereotyped behavior ($p = 0.0392$) and between max depth and ADOS social interactions ($p = 0.0082$). For the right intraparietal sulcus, the mean depth was negatively correlated with the CARS ($p = 0.0307$), ADOS ($p = 0.0198$), and ADOS social interactions ($p = 0.0181$) scores and positively correlated with Vineland daily living skills score ($p = 0.0449$). A trend towards positive correlation was observed between the mean depth of the left medial frontal

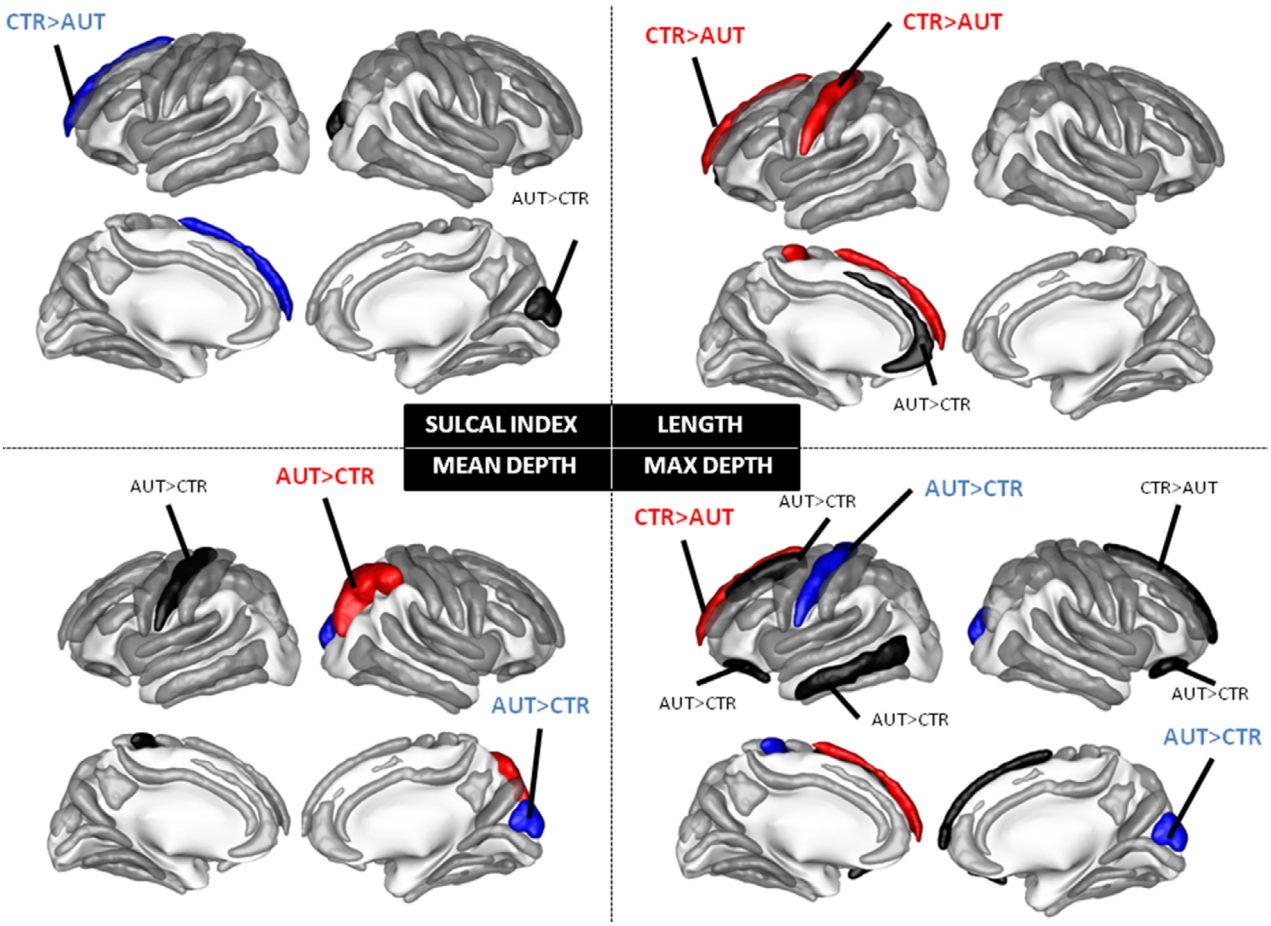

Fig. 3. Main effect of diagnostic group on sulcal shape descriptors: sulcal index, length, maximum depth and mean depth. The sulci in red have a $p < 0.05/21$ i.e., $p < 0.05$ after Bonferroni correction, the sulci in blue have a $p < 0.01$ uncorrected and the sulci in black have a $p < 0.05$ uncorrected, see text for details.

sulcus and the ADOS stereotyped behavior ($p = 0.0552$) score. A significant correlation was also found for the sulci showing trends towards differences between groups. The max depth of the right medial frontal sulcus was positively correlated with ADI social interactions ($p = 0.0290$), and negatively with Vineland ($p = 0.0440$) and Vineland daily living skills ($p = 0.0274$). Also, the max depth of the left superior frontal sulcus was negatively correlated with the ADOS stereotyped behavior ($p = 0.0406$) score.

4. Discussion

This work presents the first analysis of a large cohort of 73 well-characterized young children with autism and matched controls through several shape descriptors of manually labeled sulci. Our findings clearly evidence a localized deficient architecture in the AUT group confined to regions that are functionally relevant with respect to cognitive deficits in ASD. Of most interest, AUT and CTR exhibit different relationships between age and structural changes in brain morphology. Such differences, observed in very young children (1.5–9 years old), support the view of an early disruption of the developmental trajectory in this pathology. Finally, it should be underlined that the different sulcal shape descriptors are correlated with the CARS and ADOS scores that are specific to the autistic pathology and index symptom severity.

4.1. Sulcal shape descriptors and volumetric measures

The combination of length, mean depth and maximum depth is of particular interest in the context of developmental disorders. The maximum depth corresponds to the deepest part of a sulcus and is thought to be where the folding of the structure has begun (Lefèvre et al., 2009; Smart and McSherry, 1986; Welker, 1990), whereas the mean depth integrates depth information all along the sulcus. The maximum depth might thus be associated with geometrical features influenced by genetic factors while mean depth is more likely to be influenced by environmental factors. These considerations are supported by recent quantitative studies of inter-subjects variation in monozygotic twins indicating increasing genetic influence with depth (Im et al., 2011; Lohmann et al., 2008). One can extend this reasoning to the length descriptor as follows. As illustrated in Fig. 2, the length of the sulcus is computed on the more external part of the sulcus, which corresponds to the part of the sulcus which depth is 0. The length should thus be influenced by environmental factors even more than the mean depth. These three descriptors collectively define a gradual description of the geometry of a sulcus following a gradient of influential factors, from genetic to environmental. The SI integrates all of this information into a single measure, thus limiting the possibility of clear-cut interpretation.

The influence of the global brain measurements such as total brain volume on local morphometric descriptors is a crucial issue that needs further clarification, with only few studies investigating this point so far. In this paper, we deal with four descriptors that may not be treated

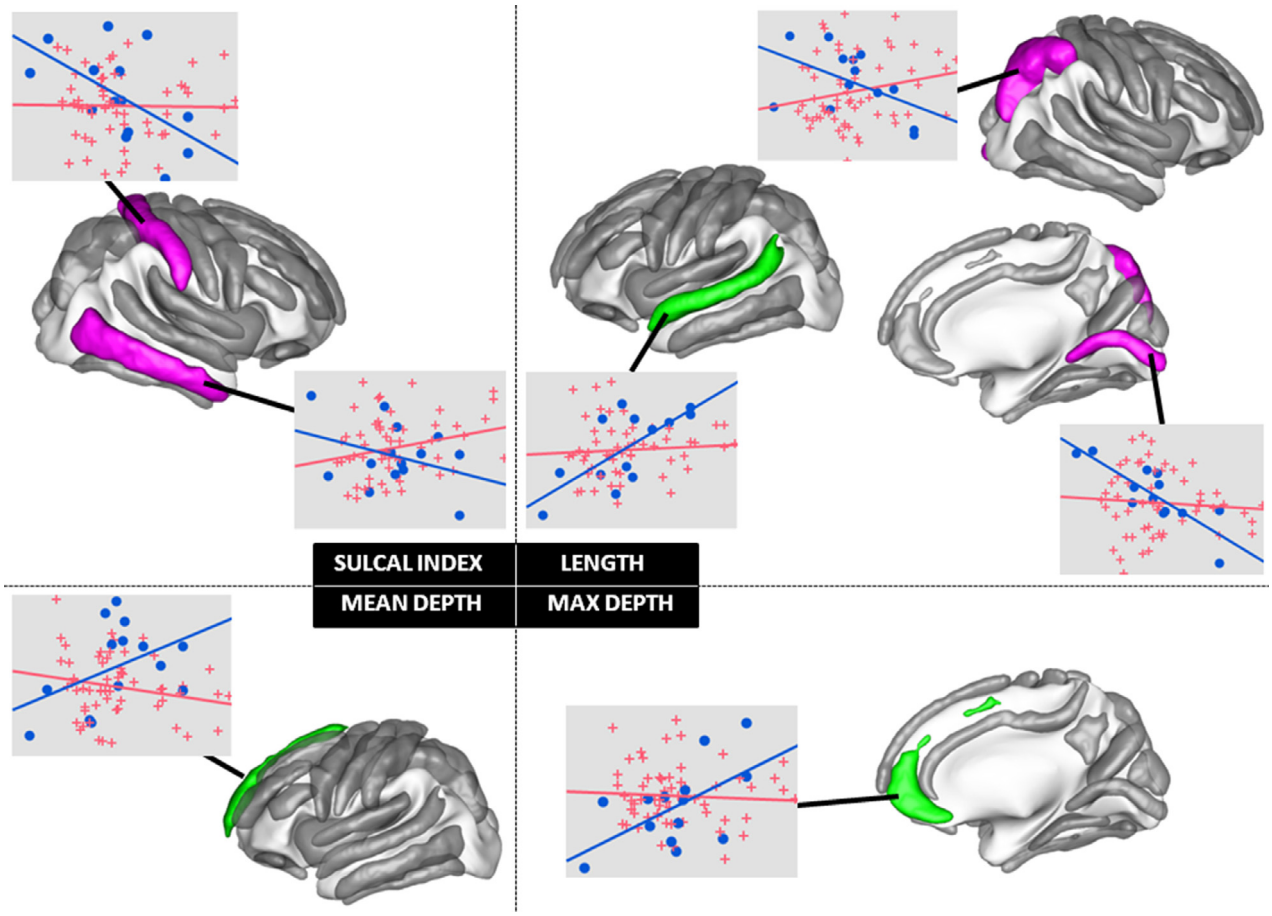

Fig. 4. Sulcal shape descriptors showing a significant age by group interaction. We show a scatter plot of each of these descriptors as a function of age (CTR as blue circles and AUT as red crosses), with the within group linear regression with age (blue line for CTR and red line for AUT).

the same way when including global covariates. For instance, including the total surface as a covariate when analyzing surface-related descriptors seems natural but may not be appropriate when analyzing depth or length measurements. Therefore, different covariates might be included according to the type of descriptors considered, then hampering a between-descriptors comparison.

Moreover, it seems plausible that the interaction between global measures and local sulcus descriptors may be different between ASD children and healthy subjects. Under this assumption, including global measures in the statistical model would bias the analysis and impede the sensitivity to the syndrome. This is why we chose an alternate strategy that consists in matching brain tissue volumes across the two groups of subjects in order to minimize such potential bias (see Section 2.1 and Table 2), thus allowing to apply the same statistical model to all four descriptors. Under this statement, spatial normalization is a way to compensate for global shape variations across individuals that has the advantage to correct for shape differences separately in each of the 3 directions (in 3D), thus yielding a more accurate correction than what would be done by including a global volumetric measurement in the statistical model, which is by essence isotropic, with a potential gain in sensitivity.

4.2. Global sulcal shape and volumetric measures

We did not detect any statistically significant increase in white or gray matter volume in young children with autism relative to controls. The absence of alteration of tissue volumes concords with some (Hazlett et al., 2005; Raznahan et al., 2013) but not all previous reports (Calderoni et al., 2012; Hazlett et al., 2011). Both the inconsistency of previous findings and the lack of significant between-group difference in any global sulcal shape measures within our young and homogeneous cohort strongly suggest that putative cortical shape abnormalities related to the autistic pathology must be spatially distributed and heterogeneous.

4.3. Local sulcal shapes in normal and autistic brains

In contrast, focusing on local sulcal descriptors revealed a clear pattern of focal anatomical disruptions in young children with autism. We report striking differences between AUT and CTR on three independent sulci and distinct evolution with age for seven independent sulci. Children with autism showed statistically significant sulcal shape abnormalities relative to CTR in the right intraparietal sulcus, the left medial frontal sulcus and the left central sulcus. This pattern resisted the conservative Bonferroni correction for multiple comparisons.

First, the mean depth of the *right intraparietal sulcus* differs between AUT and CTR. This result is similar to the larger depth reported in Asperger patients (Nordahl et al., 2007). Interestingly, others have reported significant alterations in the other indices (length; (Shokouhi and Williams, 2012); coordinates in standardized space (Levitt et al., 2003); cortical thickness: (Raznahan et al., 2013)) for the same sulcus. Altogether, these results highlight the importance of structural changes in the intraparietal sulcus related to ASD.

Second, both sulcal length and max depth were reduced in young autistic children for the *left medial frontal sulcus*. An increased cortical thickness bilaterally in an extended part of the superior frontal gyrus has been previously reported by the sole fine-grained study of cortical

structure in a population similar to ours (Raznahan et al., 2013). Of interest, this study found that the increased thickness in the right medial frontal region was clearly less pronounced than that in the left hemisphere, thus supporting the current data.

Third, the *left central sulcus* presents a significant reduction in sulcus length in AUT. Both sulcus mean and max depth indices show only a trend towards deeper fold in AUT. Note that morphological differences concerning this sulcus are the most consistently reported in the literature (see the meta-analysis of Nickl-Jockschat et al., 2012). More importantly, results relative to this sulcus illustrate the importance of our approach based on several morphological indices. The geometrical abnormality for this sulcus in AUT children is a combination of significantly deeper and shorter structure. Variations in these two complementary geometrical attributes impact the surface area of the fold in opposite ways such that the resulting difference in the SI descriptor becomes too small to be detected as in previous studies based on gyrification index (Kates et al., 2009; Wallace et al., 2013). This demonstrates the superiority of our approach compared to surface-based measurements computed on each vertex of the cortex.

Remarkably, these three abnormalities in sulcal anatomy are located in regions that are pertinent for some aspects of human cognition that are impacted in ASD. The right intraparietal sulcus is implicated in visual attention (Culham et al., 1998) as well as in social cognitive function through its role in imitation and the mirror neuron system (Williams, 2008). The left medial prefrontal cortex is involved in social judgment and is poorly functioning in autism (Watanabe et al., 2012). Lastly, the observation of abnormal geometry of the left central sulcus may relate to known motor impairments in autism (e.g., Müller et al., 2001).

4.4. The effect of age on sulcal shape in normal and autistic brains

In a small group of sulci, we found a salient difference between autistic and control brains regarding the developmental time course of sulcal shapes. Normal brains are characterized by a strong correlation between age and shape descriptors for four sulci (see Fig. 4). Autistic brains did not show such relationship, the shape descriptors remaining roughly constant over the 7–8 years spanned by our population.

These results on the age effects upon sulcal shape descriptors, and their differences between normal and autistics brains, shed a new light on the development of brain morphology. First, we can divide our sample of age-dependent sulci in two categories. Sulci showing a negative correlation with age (right calcarine sulcus, post-central sulcus and intraparietal sulcus) are known to appear before 30 weeks of gestational age, whereas sulci with positive correlation (left medial frontal sulcus, left superior temporal sulcus and the right internal frontal sulcus) emerge only after 30 weeks in typically developing children (Chi et al., 1977; Jessica Dubois et al., 2008a). Furthermore, this pattern of results is coherent with studies suggesting that cortical thickness evolves with a complex and heterogeneous pattern of maturation across the whole cortex, each area reaching a peak at different ages and then decreasing to an asymptotic level (Raznahan et al., 2011; Shaw et al., 2008). When comparing with these observations, it appears that the first group of sulci belongs to cortical regions (pre- and post-central gyri, medial occipital and parietal regions) that reach their mature stage earlier than the frontal and temporal regions where we find, instead, a positive correlation. Moreover, the difference in the correlation with age between left and right intraparietal sulci, is also consistent with the idea that right sulcus develops and matures earlier (Gilmore et al., 2012; Shaw et al., 2008). Of interest, the current pattern of correlations captures the fact that these sulci are in either the rising or the falling phase of their development. Secondly, mean and max depth sulcus shape descriptors show an interaction with age only for two sulci (left medial frontal and right internal frontal sulci) that are located in the frontal lobe which maturates last (Shaw et al., 2008). Therefore, in our population of young children, the depth, but not the length of the sulci is not influenced by age in cortical regions that are supposed to be already mature. Our results are thus in accordance with quantitative (Im et al., 2011; Lohmann et al., 2008) and theoretical (Van Essen, 1997) considerations regarding the greater genetic influence of deeper parts of the major sulci of the cortex compared to more external regions and less deep folds. In addition, they suggest that sulcal shape descriptors might reflect the maturational processes occurring in the healthy brain during childhood and adolescence such as experience-dependent molding of the architecture of cortical columns, elimination of synapses and proliferation of myelin (Casey et al., 2005; Shaw et al., 2008; White et al., 2010).

An important observation is that none of the descriptors associated with these particular sulci show a significant correlation with age in the AUT group. Our study suggests a focal pattern of cortical maturation abnormalities in ASD that concern regions that are involved in social cognition (e.g. medial prefrontal, lateral temporal, and parietal cortices) and some aspects of executive function (dorsolateral prefrontal cortices) (e.g., Mason et al., 2008). This lack of correlation with age in ASD group echoes with previous studies that found significant age-effects on cortical thickness in temporal, frontal or parietal lobes in CTR groups only (Doyle-Thomas et al., 2013; Raznahan et al., 2010; Scheel et al., 2011) on older participants than in the current work. Opposite results have also been reported however in some studies evidencing a thinner cortex with increasing age in the ASD group (Misaki et al., 2012; Wallace et al., 2010). Nevertheless, these differences highlight the fact that morphological abnormalities could evolve over the whole lifespan and that future studies shall consider age by group interactions in deciphering neural correlates of ASD.

4.5. Correlation between sulcal shape descriptors and severity scores

Morphometric descriptors of sulci are associated with more severe impairments related to the autistic pathology. To be noted, our population of autistic children was highly homogeneous for age and diagnosis. Nevertheless, for all sulci exhibiting between-groups difference, we found a significant correlation between one or several sulcal shape descriptors and the behavioral assessments. More specifically ADOS social interaction scores are correlated with depth of both right intraparietal and left central sulci while the ADOS stereotyped behavior scores correlated with depth of the left central sulcus and left superior frontal sulcus. Interestingly significant effects are observed only for the depth indices (either mean or max). As discussed above, differences in depth descriptors might signal abnormal developmental events occurring earlier than those impacting sulcal length. This would support the hypothesis of a departure from typical cortical developmental trajectory occurring very early in ASD (e.g., Courchesne et al., 2007).

Moreover, autism severity as evaluated by both CARS and ADOS is negatively correlated with the depth of the right intraparietal sulcus. A positive correlation would be expected under the assumption that this morphometric index varies continuously from control children to more severe ASD patients. Indeed, a negative correlation suggests a discontinuity that might be related to the complex and indirect link between anatomical and behavioral underpinnings, as e.g., in the presence of a genetic factor (Molko et al., 2003). Interestingly, several studies show involvement of the intraparietal sulcus in particular in eye gaze direction (e.g., Hoffman and Haxby, 2000) and in spatial attention (e.g., Corbetta et al., 1998). These activities provide information necessary for social interactions including information about identity, mood, level of interest and direction of interest (Haxby et al., 2002). Our data could thus pinpoint an early anatomical morphological index of the social interaction deficiency that is a hallmark of the autistic pathology.

5. Conclusion

In essence, in this study, we presented a new single-site cohort of young children with autism and matched controls that were all screened by the same medical staff. Despite unbalanced sample size across AUT and CTR groups, the use of sulcus-based morphometric descriptors nevertheless allowed us to compare a set of complementary geometrical attributes of the same anatomical entities between AUT and CTR children. To our knowledge, this is the first study in ASD involving fine-scale sulcus nomenclature through automatic extraction and manual identification by an expert. It is also the first report of significant difference in group by age interaction in sulcal-based morphometry analysis at sub-lobar scale. Note that the statistics for this interaction were not corrected for multiple testing and current results must thus be considered with caution.

Additionally, the observed sulcal abnormalities were localized in regions where cortical thickness increase has previously been reported and were supported by significant correlations with several severity scores. Taken together, our results underlie the salience of combining several shape descriptors in the context of autistic spectrum disorders and strongly suggest that sulcal shape differences could be the signature of disrupted maturational processes that affect this pathology.

Acknowledgments

This work was supported by a grant from Fondation de France (OTP 38872) and from Fondation Orange (S1 2013-050).

Supplementary material

Supplementary material associated with this article can be found, in the online version, at doi:10.1016/j.nicl.2014.03.008.

References

Alemán-Gómez, Y., Janssen, J., Schnack, H., Balaban, E., Pina-Camacho, L., Alfaro-Almagro, F. et al, 2013. The human cerebral cortex flattens during adolescence. Journal of Neuroscience: the Official Journal of the Society for Neuroscience 33, 15004–10. http://dx.doi.org/10.1523/JNEUROSCI.1459-13.2013, 24048830.

Amaral, D.G., Schumann, C.M., Nordahl, C.W., 2008. Neuroanatomy of autism. Trends in Neurosciences 31, 137–45. http://dx.doi.org/10.1016/j.tins.2007.12.005, 18258309.

American Psychiatric Association2000. Diagnostic and Statistical Manual of Mental Disorders: DSM-IV-TR. Springer.

Anagnostou, E., Taylor, M.J., 2011. Review of neuroimaging in autism spectrum disorders: what have we learned and where we go from here. Molecular Autism 2, 4. http://dx.doi.org/10.1186/2040-2392-2-4.

Awate, S.P., Win, L., Yushkevich, P., 2008. 3D cerebral cortical morphometry in autism: increased folding in children and adolescents in frontal, parietal, and temporal lobes. Medical image computing and computer-assisted intervention : MICCAI 11, 559–67, 18979791.

Belmonte, M.K., Allen, G., Beckel-Mitchener, A., Boulanger, L.M., Carper, R.A., Webb, S.J., 2004. Autism and abnormal development of brain connectivity. Journal of Neuroscience: the Official Journal of the Society for Neuroscience 24, 9228–31. http://dx.doi.org/10.1523/JNEUROSCI.3340-04.2004, 15496656.

Bonilha, L., Cendes, F., Rorden, C., Eckert, M., Dalgalarrondo, P., Li, L.M. et al, 2008. Gray and white matter imbalance—typical structural abnormality underlying classic autism? Brain & Development 30, 396–401. http://dx.doi.org/10.1016/j.braindev.2007.11.006, 18362056.

Cachia, A., Paillère-Martinot, M.-L., Galinowski, A., Januel, D., de Beaurepaire, R., Bellivier, F. et al, 2008. Cortical folding abnormalities in schizophrenia patients with resistant auditory hallucinations. NeuroImage 39, 927–35. http://dx.doi.org/10.1016/j.neuroimage.2007.08.049, 17988891.

Calderoni, S., Retico, A., Biagi, L., Tancredi, R., Muratori, F., Tosetti, M., 2012. Female children with autism spectrum disorder: an insight from mass-univariate and pattern classification analyses. Neuroimage 59, 1013–22. http://dx.doi.org/10.1016/j.neuroimage.2011.08.070, 21896334.

Casey, B.J., Tottenham, N., Liston, C., Durston, S., 2005. Imaging the developing brain: what have we learned about cognitive development? Trends in Cognitive Sciences 9, 104–10. http://dx.doi.org/10.1016/j.tics.2005.01.011, 15737818.

Chen, R., Jiao, Y., Herskovits, E.H., 2011. Structural MRI in autism spectrum disorder. Pediatric Research 69, 63R–68R. http://dx.doi.org/10.1203/PDR.0b013e318212c2b3, 21289538.

Chi, J.G., Dooling, E.C., Gilles, F.H., 1977. Gyral development of the human brain. Annals of Neurology 1, 86–93, 560818.

Corbetta, M., Akbudak, E., Conturo, T.E., 1998. A common network of functional areas for attention and eye movements. Neuron 21, 761–73. http://dx.doi.org/10.1016/S0896-6273(00)80593-0, 9808463.

Courchesne, E., Pierce, K., Schumann, C.M., Redcay, E., Buckwalter, J.A., Kennedy, D.P. et al, 2007. Mapping early brain development in autism. Neuron 56, 399–413. http://dx.doi.org/10.1016/j.neuron.2007.10.016, 17964254.

Culham, J.C., Brandt, S.a., Cavanagh, P., Kanwisher, N.G., Dale, A.M., Tootell, R.B., 1998. Cortical fMRI activation produced by attentive tracking of moving targets. Journal of Neurophysiology 80, 2657–70.

Cykowski, M.D., Coulon, O., Kochunov, P.V., Amunts, K., Lancaster, J.L., Laird, A.R. et al, 2008. The central sulcus: an observer-independent characterization of sulcal landmarks and depth asymmetry. Cerebral Cortex (New York, N.Y.: 1991) 18, 1999–2009. http://dx.doi.org/10.1093/cercor/bhm224, 18071195.

Doyle-Thomas, K.A., Duerden, E.G., Taylor, M.J., Lerch, J.P., Soorya, L.V., Wang, A.T. et al, 2013. Effects of age and symptomatology on cortical thickness in autism spectrum disorders. Research in autism spectrum disorders 7, 141–50.

Dubois, J., Benders, M., Borradori-Tolsa, C., Cachia, A., Lazeyras, F., Ha-Vinh, Leuchter R. et al, 2008. Primary cortical folding in the human newborn: an early marker of later functional development. Brain: a Journal of Neurology 131, 2028–41. http://dx.doi.org/10.1093/brain/awn137, 18587151.

Dubois, J., Benders, M., Cachia, A., Lazeyras, F., Ha-Vinh, Leuchter R., Sizonenko, S.V. et al, 2008. Mapping the early cortical folding process in the preterm newborn brain. Cerebral Cortex (New York, N.Y.: 1991) 18, 1444–54. http://dx.doi.org/10.1093/cercor/bhm180, 17934189.

Ecker, C., Marquand, A., Mourão-Miranda, J., Johnston, P., Daly, E.M., Brammer, M.J. et al, 2010. Describing the brain in autism in five dimensions—magnetic resonance imaging-assisted diagnosis of autism spectrum disorder using a multiparameter classification approach. Journal of Neuroscience: the Official Journal of the Society for Neuroscience 30, 10612–23. http://dx.doi.org/10.1523/JNEUROSCI.5413-09.2010, 20702694.

Garel, C., Chantrel, E., Brisse, H., Elmaleh, M., Luton, D., Oury, J.F. et al, 2001. Fetal cerebral cortex: normal gestational landmarks identified using prenatal MR imaging. AJNR. American Journal of Neuroradiology 22, 184–9, 11158907.

Germanaud, D., Lefèvre, J., Toro, R., Fischer, C., Dubois, J., Hertz-Pannier, L. et al, 2012. Larger is twistier: spectral analysis of gyrification (SPANGY) applied to adult brain size polymorphism. Neuroimage 63, 1257–72. http://dx.doi.org/10.1016/j.neuroimage.2012.07.053, 22877579.

Gilmore, J.H., Shi, F., Woolson, S.L., Knickmeyer, R.C., Short, S.J., Lin, W. et al, 2012. Longitudinal development of cortical and subcortical gray matter from birth to 2 years. Cerebral Cortex (New York, N.Y.: 1991) 22, 2478–85. http://dx.doi.org/10.1093/cercor/bhr327, 22109543.

Hadjikhani, N., Joseph, R.M., Snyder, J., Tager-Flusberg, H., 2006. Anatomical differences in the mirror neuron system and social cognition network in autism. Cerebral Cortex (New York, N.Y.: 1991) 16, 1276–82, 16306324.

Hansen, P.E., Ballesteros, M.C., Soila, K., Garcia, L., Howard, J.M., 1993. MR imaging of the developing human brain. Part 1. Prenatal development. Radiographics: a Review Publication of the Radiological Society of North America, Inc 13, 21–36. http://dx.doi.org/10.1148/radiographics.13.1.8426929, 8426929.

Hardan, A.Y., Jou, R.J., Keshavan, M.S., Varma, R., Minshew, N.J., 2004. Increased frontal cortical folding in autism: a preliminary MRI study. Psychiatry Research 131, 263–8. http://dx.doi.org/10.1016/j.pscychresns.2004.06.001, 15465295.

Haxby, J.V., Hoffman, E.A., Gobbini, M.I., 2002. Human neural systems for face recognition and social communication. Biological Psychiatry 51, 59–67. http://dx.doi.org/10.1016/S0006-3223(01)01330-0, 11801231.

Hazlett, H.C., Poe, M., Gerig, G., Smith, R.G., 2005. Magnetic resonance imaging and head circumference study of brain size in autism: birth through age 2 years. Archives of General Psychiatry 62, 1366–76. http://dx.doi.org/10.1001/archpsyc.62.12.1366, 16330725.

Hazlett, H.C., Poe, M.D., Gerig, G., Styner, M., Chappell, C., Smith, R.G. et al, 2011. Early brain overgrowth in autism associated with an increase in cortical surface area before age 2 years. Archives of General Psychiatry 68, 467–76. http://dx.doi.org/10.1001/archgenpsychiatry.2011.39, 21536976.

Hoffman, E.A., Haxby, J.V., 2000. Distinct representations of eye gaze and identity in the distributed human neural system for face perception. Nature Neuroscience 3, 80–4. http://dx.doi.org/10.1038/71152, 10607399.

Hyde, K.L., Samson, F., Evans, A.C., Mottron, L., 2010. Neuroanatomical differences in brain areas implicated in perceptual and other core features of autism revealed by cortical thickness analysis and voxel-based morphometry. Human Brain Mapping 31, 556–66, 19790171.

Im, K., Lee, J.-M., Seo, S.W., Hyung, Kim S., Kim, S.I., Na, D.L., 2008. Sulcal morphology changes and their relationship with cortical thickness and gyral white matter volume in mild cognitive impairment and Alzheimer's disease. Neuroimage 43, 103–13. http://dx.doi.org/10.1016/j.neuroimage.2008.07.016, 18691657.

Im, K., Pienaar, R., Lee, J.-M., Seong, J.-K., Choi, Y.Y., Lee, K.H. et al, 2011. Quantitative comparison and analysis of sulcal patterns using sulcal graph matching: a twin study. Neuroimage 57, 1077–86. http://dx.doi.org/10.1016/j.neuroimage.2011.04.062, 21596139.

Kates, W.R., Ikuta, I., Burnette, C.P., 2009. Gyrification patterns in monozygotic twin pairs varying in discordance for autism. Autism Research: Official Journal of the International Society for Autism Research 2, 267–78. http://dx.doi.org/10.1002/aur.98, 19890876.

Lai, M.-C., Lombardo, M.V., Suckling, J., Ruigrok, A.N.V., Chakrabarti, B., Ecker, C. et al, 2013. Biological sex affects the neurobiology of autism. Brain: a Journal of Neurology 136, 2799–815. http://dx.doi.org/10.1093/brain/awt216, 23935125.

Lefèvre, J., Leroy, F., Khan, S., Dubois, J., Huppi, P.S., Baillet, S. et al, 2009. Identification of growth seeds in the neonate brain through surfacic Helmholtz decomposition. Information Processing in Medical imaging: Proceedings of the ... Conference 21, 252–63, 19694268.

Levitt, J.G., Blanton, R.E., Smalley, S., Thompson, P.M., Guthrie, D., McCracken, J.T. et al, 2003. Cortical sulcal maps in autism. Cerebral Cortex (New York, N.Y.: 1991) 13, 728–35. http://dx.doi.org/10.1093/cercor/13.7.728, 12816888.

Lohmann, G., von Cramon, D.Y., Colchester, A.C.F., 2008. Deep sulcal landmarks provide an organizing framework for human cortical folding. Cerebral Cortex (New York, N.Y.: 1991) 18, 1415–20. http://dx.doi.org/10.1093/cercor/bhm174, 17921455.

Lord, C., Risi, S., Lambrecht, L., Cook, E.H., Leventhal, B.L., DiLavore, P.C. et al, 2000. The Autism Diagnostic Observation Schedule—Generic: a standard measure of social and communication deficits associated with the spectrum of autism. Journal of Autism and Developmental Disorders 30, 205–23. http://dx.doi.org/10.1023/A:1005592401947, 11055457.

Lotspeich, L.J., Kwon, H., Schumann, C.M., Fryer, S.L., Goodlin-Jones, B.L., Buonocore, M.H. et al, 2004. Investigation of neuroanatomical differences between autism and Asperger syndrome. Archives of General Psychiatry 61, 291–8. http://dx.doi.org/10.1001/archpsyc.61.3.291, 14993117.

Mak-Fan, K.M., Taylor, M.J., Roberts, W., Lerch, J.P., 2011. Measures of cortical grey matter structure and development in children with autism spectrum. Disorder. Journal of Autism and Developmental Disorders 42, 419–27.

Mangin, J.-F., Jouvent, E., Cachia, A., 2010. In-vivo measurement of cortical morphology: means and meanings. Current Opinion in Neurology 23, 359–67, 20489617.

Mangin, J.-F., Rivière, D., Cachia, A., Duchesnay, E., Cointepas, Y., Papadopoulos-Orfanos, D. et al, 2004. Object-based morphometry of the cerebral cortex. IEEE Transactions on Medical imaging 23, 968–82. http://dx.doi.org/10.1109/TMI.2004.831204, 15338731.

Mangin, J.-F., Rivière, D., Cachia, A., Duchesnay, E., Cointepas, Y., Papadopoulos-Orfanos, D. et al, 2004. A framework to study the cortical folding patterns. Neuroimage 23 (Suppl. 1), S129–S138. http://dx.doi.org/10.1016/j.neuroimage.2004.07.019.

Mangin, J.-F., Rivière, D., Coulon, O., Poupon, C., Cachia, A., Cointepas, Y. et al, 2004. Coordinate-based versus structural approaches to brain image analysis. Artificial intelligence in Medicine 30, 177–97. http://dx.doi.org/10.1016/S0933-3657(03)00064-2, 14992763.

Mason, R.A., Williams, D.L., Kana, R.K., 2008. Theory of mind disruption and recruitment of the right hemisphere during narrative comprehension in autism. Neuropsychologia 46, 269–80. http://dx.doi.org/10.1016/j.neuropsychologia.2007.07.018, 17869314.

Misaki, M., Wallace, G.L., Dankner, N., Martin, A., Bandettini, P.A., 2012. Characteristic cortical thickness patterns in adolescents with autism spectrum disorders: interactions with age and intellectual ability revealed by canonical correlation analysis. NeuroImage 60, 1890–901. http://dx.doi.org/10.1016/j.neuroimage.2012.01.120, 22326986.

Molko, N., Cachia, A., Rivière, D., Mangin, J.-F., Bruandet, M., Le, Bihan D. et al, 2003. Functional and structural alterations of the intraparietal sulcus in a developmental dyscalculia of genetic origin. Neuron 40, 847–58. http://dx.doi.org/10.1016/S0896-6273(03)00670-6, 14622587.

Müller, R.A., Pierce, K., Ambrose, J.B., 2001. Atypical patterns of cerebral motor activation in autism: a functional magnetic resonance study. Biological Psychiatry 49, 665–76. http://dx.doi.org/10.1016/S0006-3223(00)01004-0, 11313034.

Nickl-Jockschat, T., Habel, U., Michel, T.M., Manning, J., Laird, A.R., Fox, P.T. et al, 2012. Brain structure anomalies in autism spectrum disorder—a meta-analysis of VBM studies using anatomic likelihood estimation. Human Brain Mapping 33, 1470–89. http://dx.doi.org/10.1002/hbm.21299, 21692142.

Nordahl, C.W., Dierker, D., Mostafavi, I., Schumann, C.M., Rivera, S.M., Amaral, D.G. et al, 2007. Cortical folding abnormalities in autism revealed by surface-based morphometry. Journal of Neuroscience: the Official Journal of the Society for Neuroscience 27, 11725–35. http://dx.doi.org/10.1523/JNEUROSCI.0777-07.2007, 17959814.

Penttilä, J., Paillére-Martinot, M.-L., Martinot, J.-L., Mangin, J.-F., Burke, L., Corrigall, R. et al, 2008. Global and temporal cortical folding in patients with early-onset schizophrenia. Journal of the American Academy of Child and Adolescent Psychiatry 47, 1125–32. http://dx.doi.org/10.1097/CHI.0b013e3181825aa7, 18725863.

Penttilä, J., Paillère-Martinot, M.-L., Martinot, J.-L., Ringuenet, D., Wessa, M., Houenou, J. et al, 2009. Cortical folding in patients with bipolar disorder or unipolar depression. Journal of Psychiatry & Neuroscience: JPN 34, 127–35, 19270763.

Perrot, M., Rivière, D., Mangin, J.-F., 2011. Cortical sulci recognition and spatial normalization. Medical image Analysis 15, 529–50. http://dx.doi.org/10.1016/j.media.2011.02.008, 21441062.

Raznahan, A., Lenroot, R., Thurm, A., Gozz, M., Hanley, A., Spence, S.J. et al, 2013. Mapping cortical anatomy in preschool aged children with autism using surface-based morphometry. NeuroImage: Clinical 2, 111–19. http://dx.doi.org/10.1016/j.nicl.2012.10.005, 24179764.

Raznahan, A., Shaw, P., Lalonde, F., Stockman, M., Wallace, G.L., Greenstein, D. et al, 2011. How does your cortex grow? Journal of Neuroscience: the Official Journal of the Society for Neuroscience 31, 7174–7. http://dx.doi.org/10.1523/JNEUROSCI.0054-11.2011, 21562281.

Raznahan, A., Toro, R., Daly, E.M., Robertson, D., Murphy, C., Deeley, Q. et al, 2010. Cortical anatomy in autism spectrum disorder: an in vivo MRI study on the effect of age. Cerebral Cortex (New York, N.Y.: 1991) 20, 1332–40. http://dx.doi.org/10.1093/cercor/bhp198, 19819933.

Rutter, M., Couteur, A., Lord, C., 2003. Autism Diagnostic Interview—Revised. Angeles, CA: Western Psychological Services, Los.

Schaer, M., Cuadra, M.B., Tamarit, L., Lazeyras, F., Eliez, S., Thiran, J.-P., 2008. A surface-based approach to quantify local cortical gyrification. I. E.E.E. Transactions on Medical Imaging 27, 161–70. http://dx.doi.org/10.1109/TMI.2007.903576.

Scheel, C., Rotarska-Jagiela, A., Schilbach, L., Lehnhardt, F.G., Krug, B., Vogeley, K. et al, 2011. Imaging derived cortical thickness reduction in high-functioning autism: key regions and temporal slope. Neuroimage 58, 391–400. http://dx.doi.org/10.1016/j.neuroimage.2011.06.040, 21749926.

Schopler, E., Reichler, R., Renner, B., The Childhood Autism Rating Scale (CARS): for diagnostic screening and classification of autism (1986)

Schumann, C.M., Bloss, C.S., Barnes, C.C., Wideman, G.M., Carper, R.A., Akshoomoff, N. et al, 2010. Longitudinal magnetic resonance imaging study of cortical development through early childhood in autism. Journal of Neuroscience: the Official Journal of the Society for Neuroscience 30, 4419–27. http://dx.doi.org/10.1523/JNEUROSCI.5714-09.2010, 20335478.

Schumann, C.M., Nordahl, C.W., 2011. Bridging the gap between MRI and postmortem research in autism. Brain Research 1380, 175–86. http://dx.doi.org/10.1016/j.brainres.2010.09.061, 20869352.

Shaw, P., Kabani, N.J., Lerch, J.P., Eckstrand, K., Lenroot, R., Gogtay, N. et al, 2008. Neurodevelopmental trajectories of the human cerebral cortex. Journal of Neuroscience: the Official Journal of the Society for Neuroscience 28, 3586–94. http://dx.doi.org/10.1523/JNEUROSCI.5309-07.2008, 18385317.

Shokouhi, M., Williams, J.H., 2012. Changes in the sulcal size associated with autism spectrum disorder revealed by sulcal morphometry. Autism Research: Official Journal of the International Society for Autism Research 5, 245–52. http://dx.doi.org/10.1002/aur.1232, 22674695.

Smart, I.H., McSherry, G.M., 1986. Gyrus formation in the cerebral cortex in the ferret. I. Description of the external changes. Journal of Anatomy 146, 141–52, 3693054.

Sparrow, S., Balla, D., Cicchetti, D., Vineland Adaptive Behavior Scales: interview edition, survey form manual (1984)

Stanfield, A.C., McIntosh, A.M., Spencer, M.D., Philip, R., Gaur, S., Lawrie, S.M., 2008. Towards a neuroanatomy of autism: a systematic review and meta-analysis of structural magnetic resonance imaging studies. European Psychiatry: the Journal of the Association of European Psychiatrists 23, 289–99. http://dx.doi.org/10.1016/j.eurpsy.2008.01.61810.1016/j.eurpsy.2008.01, 61910.1016/j.eurpsy.2008.01.62010.1016/j.eurpsy.2007.05.006] [Pubmed: 17765485].

Stevenson, R.A., 2012. Using functional connectivity analyses to investigate the bases of autism spectrum disorders and other clinical populations. Journal of Neuroscience: the Official Journal of the Society for Neuroscience 32, 17933–4. http://dx.doi.org/10.1523/JNEUROSCI.4515-12.2012, 23238709.

Su, S., White, T., Schmidt, M., 2013. Geometric computation of human gyrification indexes from magnetic resonance images. Human Brain Mapping 34, 1230–44. http://dx.doi.org/10.1002/hbm.21510, 22331577.

Toal, F., Daly, E.M., Page, L., Deeley, Q., Hallahan, B., Bloemen, O. et al, 2010. Clinical and anatomical heterogeneity in autistic spectrum disorder: a structural MRI study. Psychological Medicine 40, 1171–81. http://dx.doi.org/10.1017/S0033291709991541, 19891805.

Toro, R., Perron, M., Pike, B., Richer, L., Veillette, S., Pausova, Z. et al, 2008. Brain size and folding of the human cerebral cortex. Cerebral Cortex (New York, N.Y.: 1991) 18, 2352–7. http://dx.doi.org/10.1093/cercor/bhm261, 18267953.

Van Essen, D.C., 1997. A tension-based theory of morphogenesis and compact wiring in the central nervous system. Nature 385, 313–18. http://dx.doi.org/10.1038/385313a0, 9002514.

Verhoeven, J.S.J., De, Cock P., Lagae, L., Sunaert, S., 2010. Neuroimaging of autism. Neuroradiology 52, 3–14, 20033797.

Wallace, G.L., Dankner, N., Kenworthy, L., Giedd, J.N., Martin, A., 2010. Age-related temporal and parietal cortical thinning in autism spectrum disorders. Brain: a Journal of Neurology 133, 3745–54. http://dx.doi.org/10.1093/brain/awq279, 20926367.

Wallace, G.L., Robustelli, B., Dankner, N., Kenworthy, L., Giedd, J.N., Martin, A., 2013. Increased gyrification, but comparable surface area in adolescents with autism spectrum disorders. Brain: a Journal of Neurology 136, 1956–67. http://dx.doi.org/10.1093/brain/awt106, 23715094.

Watanabe, T., Yahata, N., Abe, O., Kuwabara, H., 2012. Diminished medial prefrontal activity behind autistic social judgments of incongruent information. PloS One 7, e39561. http://dx.doi.org/10.1371/journal.pone.0039561, 22745788.

Welker, W., 1990. Why does cerebral cortex fissure and fold?, in, in: Jones, E.G., Peters, A. (Eds.), Cerebral Cortex. Springer, pp. 3–136.

White, T., Su, S., Schmidt, M., Kao, C.-Y., Sapiro, G., 2010. The development of gyrification in childhood and adolescence. Brain and Cognition 72, 36–45. http://dx.doi.org/10.1016/j.bandc.2009.10.009, 19942335.

Williams, J.H.G., 2008. Self–other relations in social development and autism: multiple roles for mirror neurons and other brain bases. Autism Research: Official Journal of the International Society for Autism Research 1, 73–90. http://dx.doi.org/10.1002/aur.15, 19360654.